Colloid Polym Sci (2015) 293:187–197
DOI 10.1007/s00396-014-3408-4

ORIGINAL CONTRIBUTION

Preparation of polymer microspheres with reactive epoxy group and amino groups as stabilizers for gold nanocolloids with recoverable catalysis

Tao Song · Meijun Zhou · Wei Liu · Guomin Bian · Yonglin Qi · Feng Bai · Xinlin Yang

Received: 9 August 2014 / Revised: 23 September 2014 / Accepted: 23 September 2014 / Published online: 4 October 2014

Abstract Narrow disperse poly(divinylbenzene-*co*-glycidyl methacrylate) (P(DVB-*co*-GMA)) microspheres with reactive epoxy group were prepared by distillation precipitation copolymerization of divinylbenzene (DVB) and glycidyl methacrylate (GMA) with benzoyl peroxide (BPO) as initiator in neat acetonitrile. The epoxy group was modified with ethylenediamine (EDA) for transferring to amino group, which was used as a stabilizer for the gold metallic nanocolloids during the in situ reduction of gold chloride trihydrate ($HAuCl_4$) with sodium borohydride ($NaBH_4$) as a reductant. The catalytic properties of the microsphere-stabilized gold nanocolloids (P(DVB-*co*-GMA)-NH_2@Au) were investigated by the reduction of aqueous 4-nitrophenol (4-NP) to 4-aminophenol (4-AnP) with $NaBH_4$ as reductant. The resultant microspheres were characterized by scanning electron microscopy (SEM), transmission electron microscopy (TEM), Fourier-transform infrared spectra (FT-IR), elemental analysis (EA), Zeta potential, X-ray photoelectron spectroscopy (XPS), inductively coupled plasma (ICP) mission spectrum, and ultraviolet–visible spectroscopy.

Keywords P(DVB-*co*-GMA) microsphere · Epoxy group · Amino group · Distillation precipitation polymerization · Gold nanocolloids

T. Song · F. Bai (✉)
Key Laboratory for Special Functional Materials of the Ministry of Education, Henan University, Kaifeng 475004, People's Republic of China
e-mail: baifengsun@gamil.com

T. Song · M. Zhou · X. Yang (✉)
Key Laboratory of Functional Polymer Materials, Ministry of Education, Institute of Polymer Chemistry, Collaborative Innovation Center of Chemical Science and Engineering (Tianjin), Nankai University, Tianjin 300071, People's Republic of China
e-mail: xlyang88@nankai.edu.cn

W. Liu (✉)
State Key Laboratory of Hollow Fiber Membrane Materials and Processes, School of Environmental and Chemical Engineering, Tianjin Polytechnic University, Tianjin 300387, People's Republic of China
e-mail: liuhuiwen217@yahoo.com

G. Bian · Y. Qi
Dynea Ltd. Co., Gaoyao City, Guangdong 526105, People's Republic of China

Introduction

The functional polymer microspheres have received much attention in many fields both from academic and industrial aspects due to their wide applications as supporting phase in chromatography, the carriers and reservoirs for controlled drug release, supporters in biomedical materials, adsorbents for the environmental protection, micro-reactor for heterogeneous catalysis, as well as the electronics [1–4]. Among them, it is interesting and essential to develop a technique to synthesize the polymer microspheres with the reactive groups, including hydroxyl [5], chloromethyl [6], and epoxy [7], which can be facilely transferred to many other groups via surface modification under mild conditions. The polymer microspheres with epoxy groups are attractive as precursor resins because they can be facilely converted by the modification reactions with nucleophiles into various functional groups, including amino [8], hydroxyl [9], aldehyde [10], and thiol [11], while the thermal stability, dimensional stability, and chemical resistance of the materials are well retained [12]. In such a way, the polymer microspheres can be endowed with novel performances for their wide applications, such as the chelating ligand for ion exchanges [13], supporters for chromatography [14], and adsorbent for blood detoxification [15]. The polymer microspheres with epoxy groups have been prepared from glycidyl methacrylate (GMA) by suspension

polymerization [16], emulsion polymerization [17], emulsification polymerization [18], dispersion polymerization [19], and surfactant reverse micelles swelling polymerization [20]. Poly(*N*-isopropylacrylamide-*co*-GMA) (P(NIPAAm-*co*-GMA)) and poly(styrene-*co*-GMA) (P(St-*co*-GMA)) microspheres were prepared by soap-free emulsion polymerization with azobis(amidinopropane) dihydrochloride (V-50) as an initiator [21, 22]. These techniques usually afford the microspheres with a broad distribution. Furthermore, the partial or complete hydrolysis of the reactive epoxy groups is still a challenge for the resultant microsphere [23], as these polymerizations are carried out in the aqueous systems.

The microspheres with amino groups have been widely used as the carriers for immobilizing and enriching monoclonal antibodies [24], the adsorbent for the treatment of hazardous wastewater containing heavy metal ions, such as Pb(II), Cd(II), Cu(II) [25], and Cr(VI) [26], respectively. It is difficult to synthesize the polymer microspheres with amino groups via the radical polymerization techniques, as Michael addition often occurs between the vinyl groups and amino groups in these systems [27]. Polyglycidyl methacrylate (PGMA) microspheres were prepared by a dispersion polymerization of GMA in the presence of poly(*N*-vinylpyrrolidone) (PVP) stabilizer, in which the epoxy groups were converted into amino groups via the surface grafting polymerization and ring-opening reaction [28].

Gold nanoparticles (Au NPs) have gained considerable attention for their wide applications in many fields, including biotechnology [29], nanotechnology [30], excellent candidates for bioconjugation with enzymes [31], and particular catalysis [32]. The microspheres grafted with functional polymer brush [33] and dendrimer [27] have been successfully utilized as stabilizer for gold metallic nanocolloids with facile and highly stable recoverable activity. However, it needs delicate design and tedious work for the synthesis of these functional polymer microspheres with multi-step procedures.

Distillation precipitation polymerization (DPP) has been developed as a facile and powerful technique for the synthesis of polymer microspheres with various functional polymer microspheres [34] and the inorganic/polymer multi-layer composite/hybrid microspheres [35]. Herein, poly(divinylbenzene-*co*-glycidyl methacrylate) (P(DVB-*co*-GMA) microspheres with epoxy groups were synthesized by DPP in acetonitrile with benzoyl peroxide (BPO) as initiator. The amino groups were afforded via the surface modification of epoxy groups with ethylene diamine (EDA). The polymer microspheres with amino groups were then used as stabilizers for the gold metallic nanocolloids during the in situ reduction of gold chloride trihydrate ($HAuCl_4$) with sodium borohydride ($NaBH_4$) as reductant. Finally, the catalytic and recoverable properties of the microsphere-stabilized gold nanocolloids were investigated via the reduction of 4-nitrophenol (4-NP) aqueous solution to 4-aminophenol (4-AnP) with $NaBH_4$ as reductant.

Experimental

Chemicals Divinylbenzene (DVB; technical grade, containing 80 % of DVB isomers, Shengli Chemical Technical Factory, Shandong, China) was washed with 5 % aqueous sodium hydroxide and water and then dried over anhydrous magnesium sulfate prior to utilization. GMA was purchased from Alfa Aesar Co. Ltd (Tianjin, China) and purified by vacuum distillation. Ethylenediamine (EDA; Alfa Aesar Co. Ltd, Tianjin, China) was used without further purification. BPO (Tianjin Chemical Reagents II Co.) was recrystallized from chloroform. Acetonitrile (Tianjin Chemical Reagents II Co.) was dried over 4 Å molecular sieves and distilled prior to use. $NaBH_4$ and 4-NP were purchased from Tianjin Chemical Reagents III Co. The aqueous solution of NaBH4 was freshly prepared before utilization. Tetrachloroauric acid trihydrate ($HAuCl_4 \cdot 3H_2O$) was obtained from Shenyang Research Institute of Nonferrous Metals, China. The other reagents and solvents were of analytical grade and used as received without further purification.

Synthesis of P(DVB-*co*-GMA) microspheres by DPP

A typical procedure for the DPP: BPO (0.04 g, 0.90 mmol, 2 wt.% relative to the total monomer), DVB (1.0 mL, 0.91 g, 7.1 mmol), and GMA (1.0 mL, 1.0 g, 7.1 mmol) (total monomer as 2.5 vol% relative to the reaction medium) were dissolved in 80 mL of acetonitrile in a dried 100 mL of two-necked flask attached with a fractionating column, Liebig condenser, and a receiver. The flask was submerged in a heating mantle, and the reaction mixture was heated from ambient temperature till boiling state within 20 min, and then the solvent began to be distilled. The initially homogeneous reaction mixture became milky white after boiling for 20 min. The reaction was stopped after 40 mL of acetonitrile was distilled from the reaction system within 90 min. After copolymerization, the resultant P(DVB-*co*-GMA) microspheres were separated by centrifugation and washed successively with anhydrous ethanol for three times. The polymer particles were dried at 50 °C in a vacuum oven till constant weight.

The procedures for the other distillation precipitation copolymerizations were similar to the typical one via varying the mass fractions of GMA in the monomer feed in the range of 0 to 0.7 (mass ratio), while the total monomer concentration, the amount of BPO, and acetonitrile were kept at the same levels as the above.

Preparation of polymer microspheres with amino groups via modification of P(DVB-*co*-GMA) with EDA

EDA was used for the modification of P(DVB-*co*-GMA) microspheres to afford amino groups on the surface. For a

representative experiment, 0.10 g of P(DVB-*co*-GMA) particles were added in 100 mL of flash containing 60.0 mL of acetonitrile and 2.50 mL of EDA. The mixture was stirred at 80 °C for 24 h. The mixture was then centrifuged, and the microspheres were washed with ethanol to remove the excess EDA for three times. The particles were denoted as P(DVB-*co*-GMA)-NH_2.

The procedures for the other chemical modifications with EDA were very similar to the representative one through altering the different mass ratios of EDA to P(DVB-*co*-GMA) microspheres, which were afforded by DPP with different GMA fractions, respectively.

Synthesis of P(DVB-***co***-GMA)-NH_2 stabilized gold nanocolloids

The Au NPs were loaded onto the gel layer and surface of the P(DVB-*co*-GMA)-NH_2 via in situ reduction of $HAuCl_4$ with $NaBH_4$ as reductant. The details of loading Au NPs were as follows: 0.10 g of P(DVB-*co*-GMA)-NH_2 microspheres (containing 0.16 mmol amino group) were suspended in 10.0 mL of deionized water in a 25-mL round flask and 0.45 mL of 0.06 M $HAuCl_4$ aqueous solution was added. Then, 10 mL of 0.05 M $NaBH_4$ aqueous solution was added dropwise under ice water bathing with stirring. The system turned purple immediately, indicating the formation of the Au NPs, and the reaction mixture was stirred further for 12 h. The resultant product was denoted as P(DVB-*co*-GMA)-NH_2@Au and purified by washing with water for three times and dried under vacuum till constant weight.

Catalytic reduction of 4-NP to 4-AnP by P(DVB-***co***-GMA)-NH_2@Au

The catalytic activity of the P(DVB-*co*-GMA)-NH_2@Au system was investigated by the reduction of 4-NP to 4-AnP using $NaBH_4$ as a model reaction. A specific experiment was carried out as follows: 0.10 mL of 4-NP aqueous solution (5 mM, 5×10^{-8} mol), 1.0 mL of $NaBH_4$ (0.20 M, 2.0×10^{-4} mol) aqueous solution, and 0.20 mL of water were mixed in a colorimetric tube. After introducing 0.05 mL of catalyst dispersion (1.0 mg/mL, 5×10^{-5} g, containing 1.3×10^{-8} mol Au) into the mixture with gentle shaking, the bright yellow solution faded gradually as the catalytic reaction proceeded. The catalytic activity was measured through an ultraviolet–visible (UV–vis) spectrophotometer with a decrease in peak at 400 nm for UV–vis absorption with a simultaneous increase in the absorption peak at 300 nm, indicating the formation of 4-AnP.

For the investigation of the recoverable catalytic activity, 0.20 mL of deionized water, 1.0 mL of newly prepared $NaBH_4$ aqueous solution (0.20 mol/L, 2.0×10^{-4} mol), and 0.10 mL of 4-NP aqueous solution (5.0 mmol/L, 5.0×10^{-8} mol) were mixed in a 4.0-mL flask and were kept at 298 K for 20 min. Then 0.20 mL of P(DVB-*co*-GMA)-NH_2@Au aqueous suspension (1.0 mg/mL, 5×10^{-5} g, containing 5.2×10^{-8} mol Au) was quickly added, and the catalytic reduction was carried out for 5 min. The conversion of the 4-NP was determined by the UV–vis spectrum with the decrease in the adsorption peak at 400 nm. After complete reduction of 4-NP, the catalysts were separated by centrifugation (1.2×10^4 rpm for 10 min) and redispersed for a new reaction system. The recovery of the catalyst was further proven by recycling it for four times.

Characterization

The morphology, particle size, and size distribution of the polymer microspheres were studied by scanning electron microscope (SEM; Shimadzu SS-550, Japan) and transmission electron microscopy (TEM; JEM 2010, Japan). All of the SEM diameters reflect an average of about 100 particles each, which were calculated according to the following formulae:

$$U = D_{\mathrm{w}}/\mathrm{D_n}$$

$$D_n = \sum_{\mathrm{i}=1}^{\mathrm{k}} \mathrm{n_i}\, D_{\mathrm{i}} / \sum_{\mathrm{i}=1}^{\mathrm{k}} \mathrm{n_i}$$

$$D_{\mathrm{w}} = \sum_{\mathrm{i}=1}^{\mathrm{k}} \mathrm{n_i} D_{\mathrm{i}}^4 / \sum_{\mathrm{i}=1}^{\mathrm{k}} \mathrm{n_i} D_{\mathrm{i}}^3$$

where, U is the polydispersity index, D_n is the number-average diameter, D_w is the weight-average diameter, N is the total number of measured particles, and D_i is the particle diameter of the determined microspheres.

Fourier-transform infrared analysis was performed with a Varian FTS6000 FT-IR spectrometer. All samples were mixed and ground with spectroscopic-grade potassium bromide, and diffuse reflectance spectra were scanned over a range of 400–4000 cm^{-1}. UV–vis spectroscopy was performed on a TU-1900 spectrometer. Elemental analysis (EA) was performed on a PerkinElmer 2400 instrument to determine the nitrogen content of the resultant polymer particles. Zeta potential analysis was checked on a zeta potential analyzer (Zeta Plus, Brookhaven Instrument Co.); contact angle of a 5-μL water on the surface was measured on a G1023-MK3 Contact Angle System (Kruss GmbH Co., Germany) equipped with DSA 10 water droplet analysis at room temperature. The nature of interaction between Au particles and functional groups on microspheres was analyzed by X-ray photoelectron spectroscopy (XPS; Kratos Axis Ultra DLD multi-technique X-ray photoelectron spectrometer) with a standard Al*Ka* excitation source (hv=1486.6 eV). The binding energy (BE) scale was calibrated by measuring C1s peak of alky carbon (BE= 284.6 eV) and the peak fitting used the freely available XPS Peak 4.1 program. Atomic emission spectrometry (AES) was

performed with inductively coupled plasma (ICP) mission spectrum on an ICP-9000 (N+M) spectrometer (USA Thermo Jarrell-Ash) to determine the loading capacity of the Au NPs.

Results and discussion

Scheme 1 illustrates the synthesis of P(DVB-*co*-GMA) microsphere with epoxy groups, the modification of EDA to incorporate the surface amino groups, and their further application as stabilizer for gold nanocolloids. In the present work, acetonitrile met the solvency conditions required for the formation of monodisperse polymer microspheres, i.e., it dissolved the monomer but precipitated the P(DVB-*co*-GMA) network.

Effect of GMA fractions in monomer feed on the morphology and size of P(DVB-*co*-GMA) microspheres

Copolymerizations of DVB and GMA were performed at 2.5 vol% of total comonomer loading relative to the whole reaction medium and 2 wt.% BPO initiator ratio to the total comonomers. Herein, the GMA fractions in the comonomer feed ranged from 0 to 0.70 in mass ratios. The SEM images of the resultant P(DVB-*co*-GMA) microspheres with different GMA fractions in monomer feed were illustrated in Fig. 1.

Figure 1a–g indicated that the resultant P(DVB-*co*-GMA) nanoparticled had spherical shape and smooth surface while the GMA fractions ranging from 0 to 0.6 (mass ratio). When

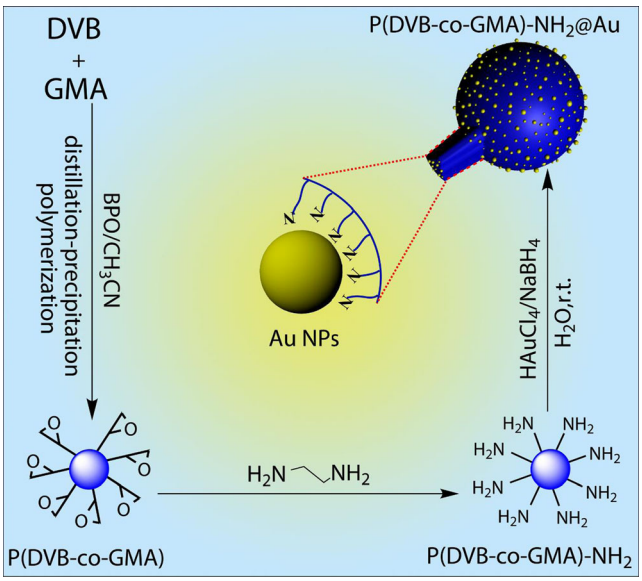

Scheme 1 Preparation of the P(DVB-*co*-GMA) microspheres with reactive surface epoxy and amino groups as stabilizer for gold metallic nanocolloids

GMA in monomer loading was increased further to 0.70, only P(DVB-*co*-GMA) particle with irregular shape and several particles were usually aggregated together as shown in Fig. 1h. This may be due to the extension of the particle nucleation under lower crosslinking degree, which was similar to the case reported in the literature [34]. Only sol was afforded in absence of any precipitate when the GMA fraction was enhanced further to 0.80. The experimental results demonstrated that the GMA fraction had significant effect on the morphology on the resultant P(DVB-*co*-GMA) networks.

Table 1 summarized the size and size distribution of P(DVB-*co*-GMA) microspheres from different GMA fractions in the monomer feed with BPO as initiator. It indicated that the diameters of the P(DVB-*co*-GMA) microspheres varied between 1.37 and 2.91 μm via altering the GMA fractions from 0 to 0.70 in the comonomer feed. The diameter had a tendency to increase with higher GMA fractions till up to 0.50. The largest size of 2.91 μm was obtained with a narrow dispersity (PDI of 1.05) when GMA fraction was 0.50. The diameters of the resultant P(DVB-*co*-GMA) microspheres tended to decrease with increasing the GMA fraction from 0.60 to 0.70. The smallest size of 1.37 μm was afforded via DPP of neat DVB in the present work. These might be originated from the lower yield of P(DVB-*co*-GMA) microspheres in the cases of lower crosslinking degrees (GMA fractions of 0.60 and 0.70), which was similar to the synthesis of poly(divinylbenzene-*co*-styrene) in our previous work [34].

The monomer reactivity ratios could be calculated from the Alfrey-Price Q and e parameters for GMA (Q_G=1.03, e_G=0.57) and styrene (Q_s=1, e_s=−0.8), respectively, according to the Alfrey-Price Q-e principle as follows:

$$r_1 = \frac{K_{11}}{K_{12}} = \frac{Q_1}{Q_2} e^{-e_1(e_1-e_2)} = 0.47 \quad (1)$$

$$r_2 = \frac{K_{22}}{K_{21}} = \frac{Q_2}{Q_1} e^{-e_2(e_2-e_1)} = 0.32 \quad (2)$$

The results show that $K_{11}<K_{12}$ and $K_{22}<K_{21}$. As a result, St are more reactive than GMA during the DPP, as it is also a typical radical polymerization. From our previous work, it was found that the reactivity of DVB was even higher than St according to the conversion of the comonomers during DPP [34]. It can be concluded that the reactivity of DVB is significantly higher than that of GMA during DPP.

The presence of epoxy groups on the surface of P(DVB-*co*-GMA) microspheres was confirmed by FT-IR spectra as shown in Fig. 2. Comparing to the FT-IR spectrum of poly(divinylbenzene) (PDVB) in Fig. 2a (a), Fig. 2a (b) had a strong peak at 1724 cm^{-1} corresponding to the carbonyl component of the ester group as well as the peaks at 845 and 910 cm^{-1} assigned to the characteristic absorption of the

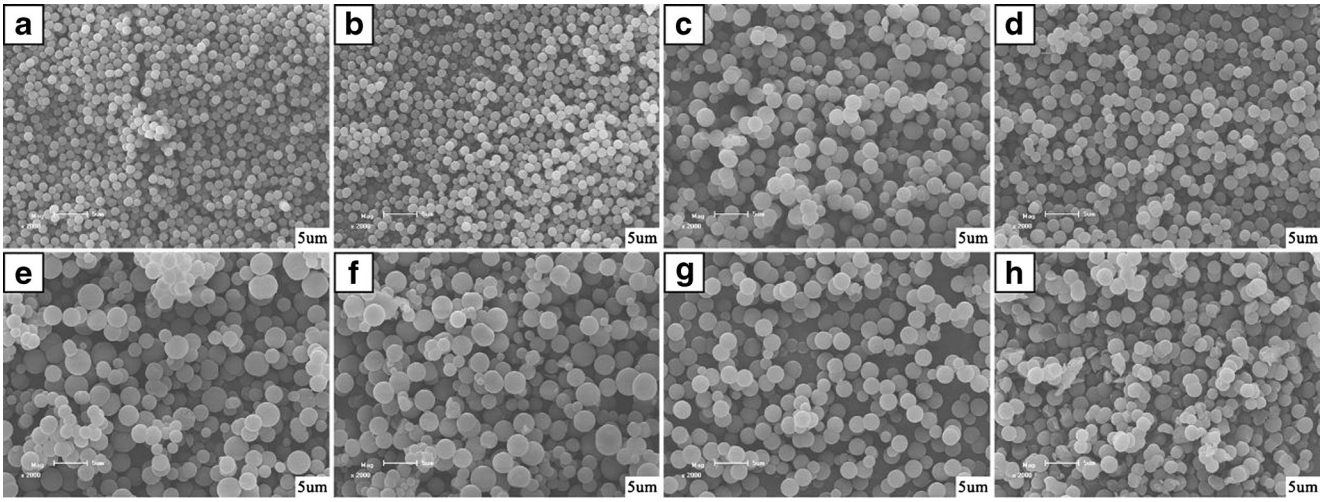

Fig. 1 SEM images of P(DVB-*co*-GMA) microspheres with different GMA fractions in monomer feed with BPO as initiator: **a** 0, **b** 0.1, **c** 0.2, **d** 0.3, **e** 0.4, **f** 0.5, **g** 0.6, and **h** 0.7

epoxy groups for the P(DVB-*co*-GMA) microsphere (with GMA fraction of 0.60 in the comonomer feed as a sample). Moreover, the characteristic peaks of the epoxy groups in the FT-IR spectrum of P(DVB-*co*-GMA) microsphere was significantly increased as shown in Fig. 2b, which implied that the loading capacity of the epoxy group was successfully incorporated onto the microspheres and enhanced with increasing GMA fraction in the copolymer, which was similar to the cases of synthesis of poly(DVB-*co*-acrylonitrile) microspheres with cyano group [36]. The epoxy groups were well retained during the DPP in acetonitrile in absence of any water molecules comparing to P(NIPAAm-*co*-GMA) and P(St-*co*-GMA) microspheres by soap-free emulsion polymerization with V-50 as initiator [21, 22], in which most epoxy groups were converted to glycol units during polymerization. As a result, it would be difficult to detect the epoxy groups on the surface of P(NIPAAm-*co*-GMA) and P(St-*co*-GMA) microspheres via FT-IR spectra in the literatures.

Table 1 The size and size distribution of P(DVB-*co*-GMA) microspheres with various GMA fractions in the comonomer feed

Entry	Fraction of GMA	BPO (g)	D_n (μm)	D_w (μm)	U
A	0	0.04	1.37	1.37	1.00
B	0.1	0.04	1.43	1.44	1.01
C	0.2	0.04	2.44	2.49	1.02
D	0.3	0.04	2.38	2.43	1.02
E	0.4	0.04	2.43	2.57	1.06
F	0.5	0.04	2.91	3.06	1.05
G	0.6	0.04	2.57	2.65	1.03
H	0.7	0.04	2.30	2.44	1.06

D_n the number average diameter, D_w the weight-average diameter, U polydispersity

Preparation of P(DVB-***co***-GMA)-NH_2 microspheres having surface amino groups via modification with EDA

The chemical modification of P(DVB-*co*-GMA) particles was performed by ring-opening reaction of the epoxy groups with EDA molecules to afford P(DVB-*co*-GMA)-NH_2 microspheres with the surface amino groups as illustrated in Scheme 1. The FT-IR spectrum of P(DVB-*co*-GMA)-NH_2 microsphere was shown in Fig. 2a (c), in which the new bands of 1604, 3310, and 3360 cm^{-1} were clearly observed assigning to the vibrations of N–H groups with the simultaneous disappearance of the bands at 845 and 910 cm^{-1} corresponding to the characteristic absorption of the epoxy groups in P(DVB-*co*-GMA) microsphere. Meanwhile, the intensities of the peaks at 1604, 3310, and 3360 cm^{-1} for the FT-IR spectra of P(DVB-*co*-GMA)-NH_2 microspheres in Fig. 2c were considerably increased with the higher GMA fractions in the comonomer feed, which were consistent with the trends of the higher epoxy groups as shown in Fig. 2b. These implied that the surface epoxy groups on P(DVB-*co*-GMA) microspheres were highly reactive and accessible for the chemical modification.

Furthermore, the zeta potentials were measured to confirm the successful incorporation of the surface amino groups on P(DVB-*co*-GMA)-NH_2 microspheres via chemical modification with EDA. Figure 3 displayed the variations of the potentials between P(DVB-*co*-GMA) and P(DVB-*co*-GMA)-NH_2 microspheres as a function of the fractions of GMA in the comonomer feed. The zeta potentials of P(DVB-*co*-GMA) microspheres were considerably decreased from −19.9 to −34.8 mV (curve a in Fig. 3) when the GMA fraction in the comonomer feed was enhanced from 0.10 to 0.70. After modification of the epoxy groups with EDA, the zeta potentials of P(DVB-*co*-GMA)-NH_2 microspheres were altered to around +20 mV (curve b in Fig. 3), which were slightly dependent on the GMA fractions in the comonomer

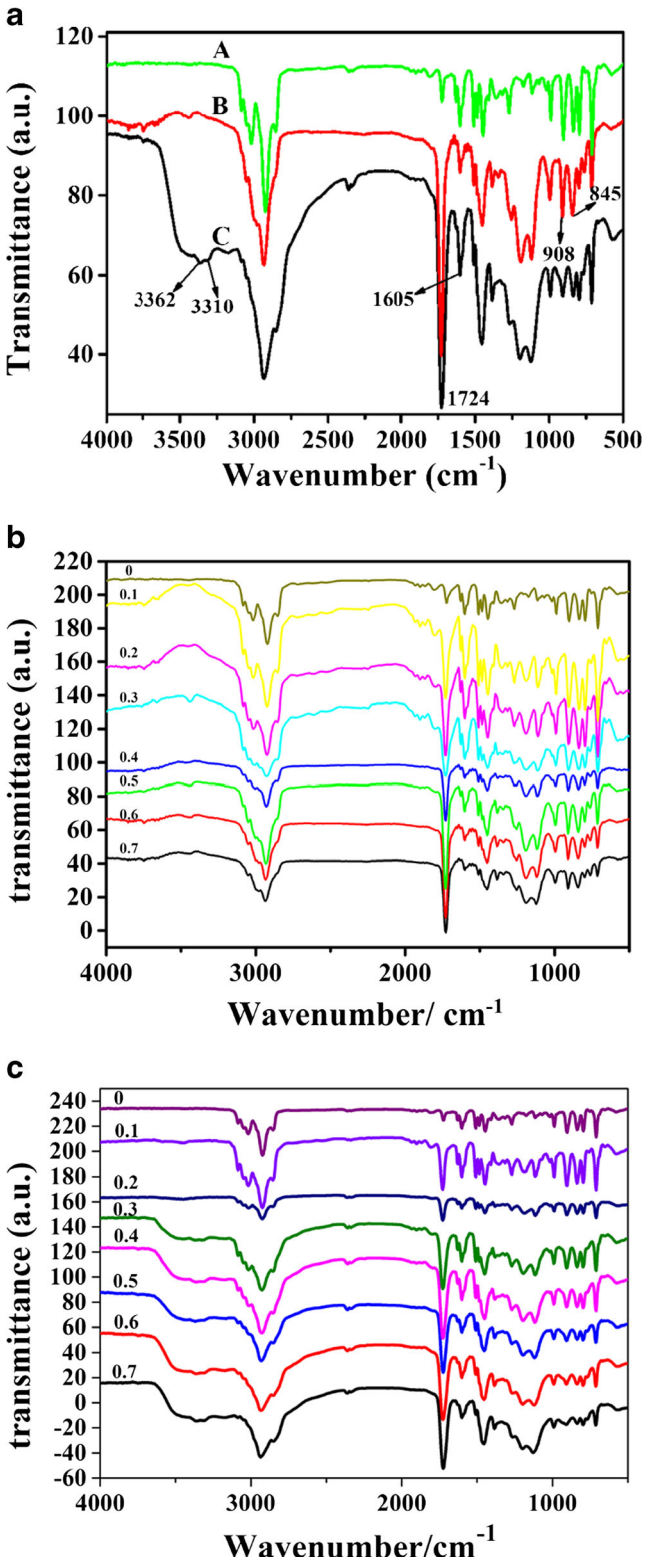

Fig. 2 FT-IR spectra of functional polymer microsphere: **a** *a* PDVB, *b* P(DVB-*co*-GMA) (GMA fraction of 0.06 in comonomer feed), and *c* P(DVB-*co*-GMA)-NH_2 from (*b*). **b** P(DVB-*co*-GMA) microspheres with the different GMA fraction in the range of 0 to 0.7 in monomer feed with BPO as initiator. **c** P(DVB-*co*-GMA)-NH_2 microspheres with the different GMA fraction in the range of 0 to 0.7 in monomer feed

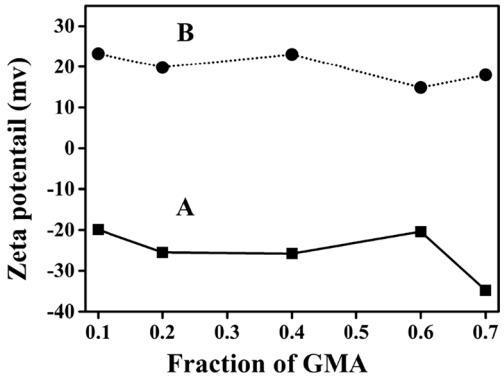

Fig. 3 Zeta potentials: *A* P(DVB-*co*-GMA) microspheres with the different GMA fraction in the range of 0 to 0.7 in monomer feed with BPO as initiator. *B* P(DVB-*co*-GMA)-NH_2 microspheres with the different GMA fraction in the range of 0 to 0.7 in monomer feed

feed. In other words, the surface of P(DVB-*co*-GMA) microsphere with negative charges were transferred to P(DVB-*co*-GMA)-NH_2 microspheres with positive surface charges, which would find potential application as delivery vector for in vitro gene transfection [37]. The surface of the polymer microspheres was gradually changed from hydrophobic to hydrophilic during the amination of the epoxy groups with EDA at 80 °C in water, which enabled good dispersion of P(DVB-*co*-GMA)-NH_2 microspheres in aqueous solution. This would provide the possibility of in situ synthesis of P(DVB-*co*-GMA)-NH_2@Au nanoparticles via the coordination of amino groups to gold atoms in the present work.

The loading capacities of the accessible epoxy groups on P(DVB-*co*-GMA) microspheres were calculated from the *CHN* EA of P(DVB-*co*-GMA)-NH_2 microspheres on a Perkin Elmer 2400 instrument. Figure 4 illustrates the relationship between the loading capacities of the accessible reactive epoxy groups on P(DVB-*co*-GMA) microspheres and the initial GMA fractions in the comonomer feedings. Figure 4 illustrates the relationship between the loading capacity of the accessible reactive epoxy groups on P(DVB-*co*-GMA) microspheres and the initial GMA fractions in the

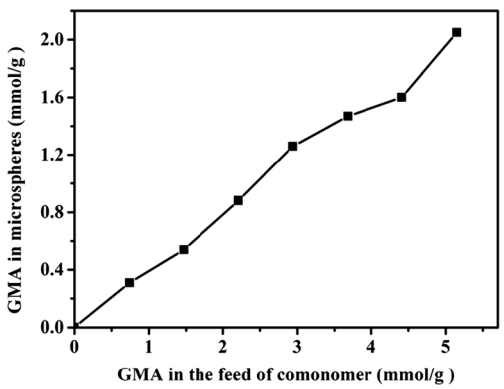

Fig. 4 The relationship between the loading capacity of the accessible epoxy groups and the GMA fractions in the commoner feed for P(DVB-*co*-GMA) microspheres via DPP

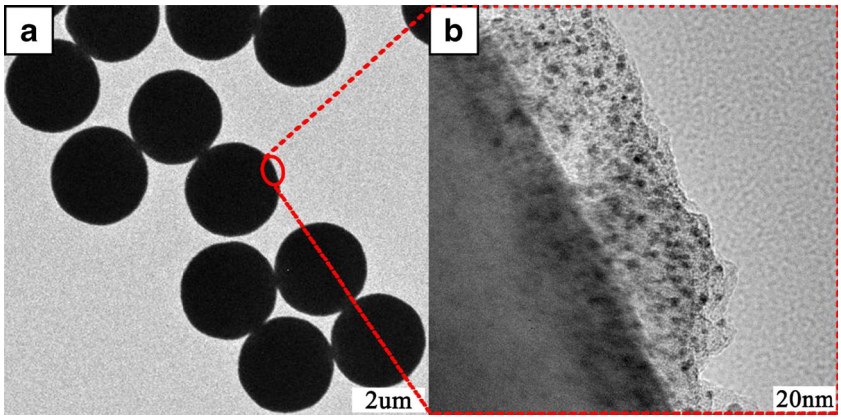

Fig. 5 TEM micrographs of P(DVB-*co*-GMA)-NH_2@Au microspheres with GMA fraction of 0.60: **a** low-magnification and **b** high-resolution TEM

comonomer feedings. The results indicated that the loading capacity of the epoxy groups on the resultant P(DVB-*co*-GMA) microspheres was a little lower than the corresponding GMA fraction in the comonomer feed, which may be originated from the higher reactivity of DVB crosslinker comparing to that of GMA functional monomer during the DPP with radical initiator. In such a system, more DVB molecules were incorporated into the inner layer than the outer layer for the resultant P(DVB-*co*-GMA) microspheres, which was similar to the case for the synthesis of P(DVB-*co*-methacrylic acid) microspheres via DPP [38]. The functional groups (hydroxyl and carboxylic acid) both on the surface and in the soft gel layer of the polymer microspheres were highly accessible with good reactivity in our previous works [5, 36]. With increasing GMA fractions in the P(DVB-*co*-GMA) microspheres, the loading capacities of the epoxy groups were significantly increased as shown in Fig. 4 with enhancing GMA fraction in the comonomer feed. As a result, the highest loading capacity with 2.05 mmol/g epoxy and amino groups were afforded for P(DVB-*co*-GMA) and P(DVB-*co*-GMA)-NH_2 microspheres with a GMA fraction of 0.70 in the comonomer feed, which would be used as the stabilizer for the gold nanocolloids in this work. The amount of epoxy groups on the surface of P(St-*co*-GMA) latex particles was calculated around 1.40 mmol/g via soap-free emulsion polymerization [22].

P(DVB-***co***-GMA)-NH_2 stabilized gold nanocolloids

It is a suitable choice of amino groups as stabilizers for metallic nanoparticles due to its complexing interaction between the nitrogen atom in amino groups with metallic atoms [39, 40]. Consequently, the gold nanocolloids were uniformly deposited onto the surface of P(DVB-*co*-GMA)-NH_2 microspheres with hydrophilic surface (GMA fraction of 0.60 in the comonomer feed as an example) by the in situ reduction of $HAuCl_4$ with $NaBH_4$ as reductant via the stabilization of the amino groups. Figure 5 shows the typical TEM micrograph of the resultant P(DVB-*co*-GMA)-NH_2@Au. It was observed more clearly in Fig. 5b with higher magnification that many deeper contrast gold nanocolloids uniformly dispersed on the surface and gel layer of P(DVB-*co*-GMA)-NH_2@Au. The formation of the gel layer on the shell of P(DVB-*co*-GMA)-NH_2 mainly originated higher reactivity of DVB crosslinker than that of GMA functional monomer during DPP. With processing polymerization, the fractions of DVB in the solution was becoming lower and lower. As a result, the core of P(DVB-*co*-GMA) microspheres was highly crosslinked and shell was slightly crosslinked, which was highly swollen in aqueous solution. As a result, P(DVB-*co*-GMA)-NH_2@Au microspheres with good dispersion of Au NPs on the surface and gel layer were synthesized by in situ reduction of $HAuCl_4$ with $NaBH_4$ as reductant via efficient coordination of amino group to gold atoms. The average diameter of the gold nanocolloids was 4.5 nm with a polydispersity index of 1.07 as summarized in Table 2. The loading capacity of the gold on P(DVB-*co*-GMA)-NH_2@Au microspheres was 5.44 % (2.76×10^{-2} mmol/g) as measured by ICP technique.

XPS is an effective method for analysis of the interaction at the interface, especially for that between the surface functional group as stabilizer and metallic nanocolloid [41, 42]. Herein,

Table 2 The size and size distribution of P(DVB-*co*-GMA)-NH_2 stabilized Au nanocolloids with the fraction of GMA at 0.6

Entry	Fraction of GMA	Nitrogen content (mmol/g)	D_n (nm)	D_w (nm)	U	Loading capacity (mg Au/g)
1	0.6	1.60	4.5	4.8	1.07	5.44

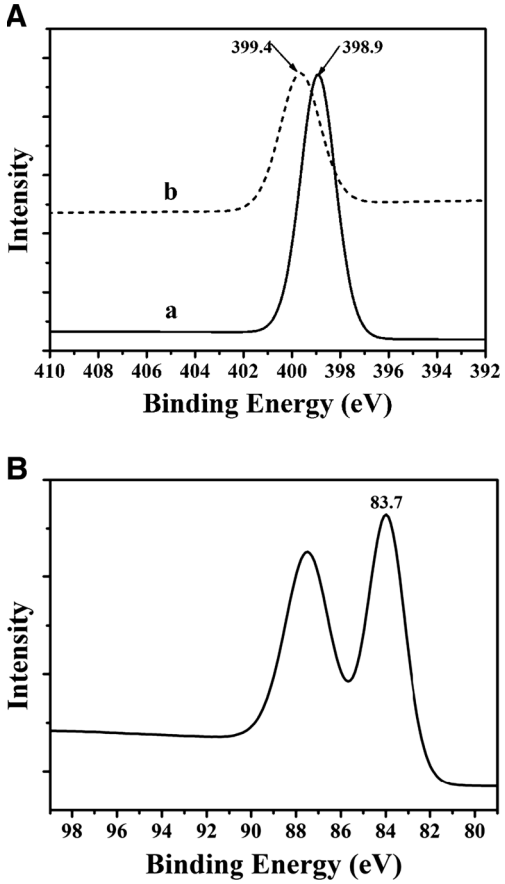

Fig. 6 XPS spectra: **A** *a* Binding energy (BE) of N_{1s} for P(DVB-*co*-GMA)-NH_2; *b* BE of N_{1s} for P(DVB-*co*-GMA)-NH_2@Au. **B** BE of $Au_{4f7/2}$ for P(DVB-*co*-GMA)-NH_2@Au

the XPS spectra were determined to confirm the complexing interaction between the amino groups and the gold atoms in P(DVB-*co*-GMA)-NH_2@Au microsphere as shown in Fig. 6, in which the BE of the saturated alkyl C_{1s} peak (BE= 284.6 eV) was used as an internal standard. The XPS spectra of N_{1s} for P(DVB-*co*-GMA)-NH_2 and P(DVB-*co*-GMA)-NH_2@Au microspheres were shown as Fig. 6A (*a*, *b*), respectively. It was observed that the BE of N_{1s} was shifted from 398.9 eV of P(DVB-*co*-GMA)-NH_2 to 399.4 eV of P(DVB-*co*-GMA)-NH_2@Au. The final-state effect was out of consideration for the gold nanocolloids in this work as the average size of Au NPs (4.53 nm) was larger than that of the final state (3–4 nm) [43]. For P(DVB-*co*-GMA)-NH_2@Au microsphere, the BE of $Au_{4f7/2}$ was shifted to 83.7 eV from 84.0 eV of standard value for the bulk gold as shown in Fig. 6B. The shifts of the BE peaks for $Au_{4f7/2}$ and N_{1s} in XPS spectra demonstrated that the supported gold nanocolloids accepted electron from the nitrogen atom via the efficient complexing interaction between the gold atoms and nitrogen atoms of the surface amino groups, which was the nature for the stabilization of gold nanocolloids in P(DVB-*co*-GMA)-NH_2@Au microsphere.

It is well-known that the metallic nanocolloids are excellent catalysts with high activity and selectivity. Therefore, the gold nanocolloids stabilized by the amino groups on the surface and gel layer of P(DVB-*co*-GMA)-NH_2@Au microsphere served as recyclable catalyst for the reduction of 4-NP to 4-AnP in aqueous solution as a model reaction. An aqueous solution of 4-NP with $NaBH_4$ has a distinct UV–vis spectral profile with an absorption maximum at 400 nm due to formation of 4-nitrophenolate anions, while the aqueous solution of the product 4-AnP has a weak peak at 310 nm [44]. With the catalytic reaction processing, the yellow color of 4-NP with absorption peak at 400 nm faded gradually together with a simultaneous development of a new absorption peak at 310 nm assigning to 4-AnP. The UV–vis spectra were determined as shown in Fig. 7a for the catalytic reaction under 298 K at different reaction times with P(DVB-*co*-GMA)-NH_2@Au as a catalyst. As the $NaBH_4$ was used in an excess amount, the catalytic reduction of 4-NP is a pseudo-first order relating to the concentration of 4-AnP. Herein, only BH_4^- is unable to reduce 4-NP to 4-AnP under the experimental conditions in absence of the stabilized gold nanocolloids, as the intensity of 4-NP at 400 nm in UV–vis absorption remained constant without any change even for tens of minutes as shown in Fig. 7b. The catalytic reaction rate was stable with a linear plot at the initial stage and then leveled off later than 15 min as shown in Fig. 7b. From the linear curve of the corresponding $\ln C_{4\text{-NP}}/C_{0,4\text{-NP}}$ vs reaction time in Fig. 7c, the apparent reaction kinetic (k) constant was calculated as 2.8×10^{-3} s^{-1} for this pseudo-first-order reaction. The high catalytic activity was mainly originated from the good dispersion of Au NPs on the surface and gel layer of P(DVB-*co*-GMA)-NH_2@Au microspheres in a highly swollen state as shown by TEM micrograph in Fig. 5b, which was easily an accessible state for 4-NP and BH_4^- reductant during the catalysis. The catalytic rate in the present work was comparative to those of the inorganic oxide-supported Au NPs for this reaction, for example, 2.5×10^{-3} s^{-1} of mesoporous titania fibers supported Au [45], 5.3×10^{-3} s^{-1} of magnetic mesoporous silica nanotube stabilized Au [46], and lower than 1.20×10^{-2} s^{-1} of imidazolium ionic liquid modified fibrous silica microsphere-loaded Au nanoparticles [47]. However, the complex procedure and residual impurities of porous inorganic architectures would limit its wide application as an efficient catalyst.

The stability and recyclability are of unique importance for the supported metallic nanocolloid as catalyst. To investigate the reusability of the P(DVB-*co*-GMA)-NH_2@Au as a recyclable catalyst, a four-time amount of the catalyst as the above procedure (2×10^{-4} g, containing 5.2×10^{-8} mol Au) was used to speed up the reaction in this work. The catalytic reduction was performed for 5 min at 298 K during each cycle. Then the catalyst was separated and recycled from the reaction system via ultra-centrifugation. As shown in Fig. 7d, the conversion

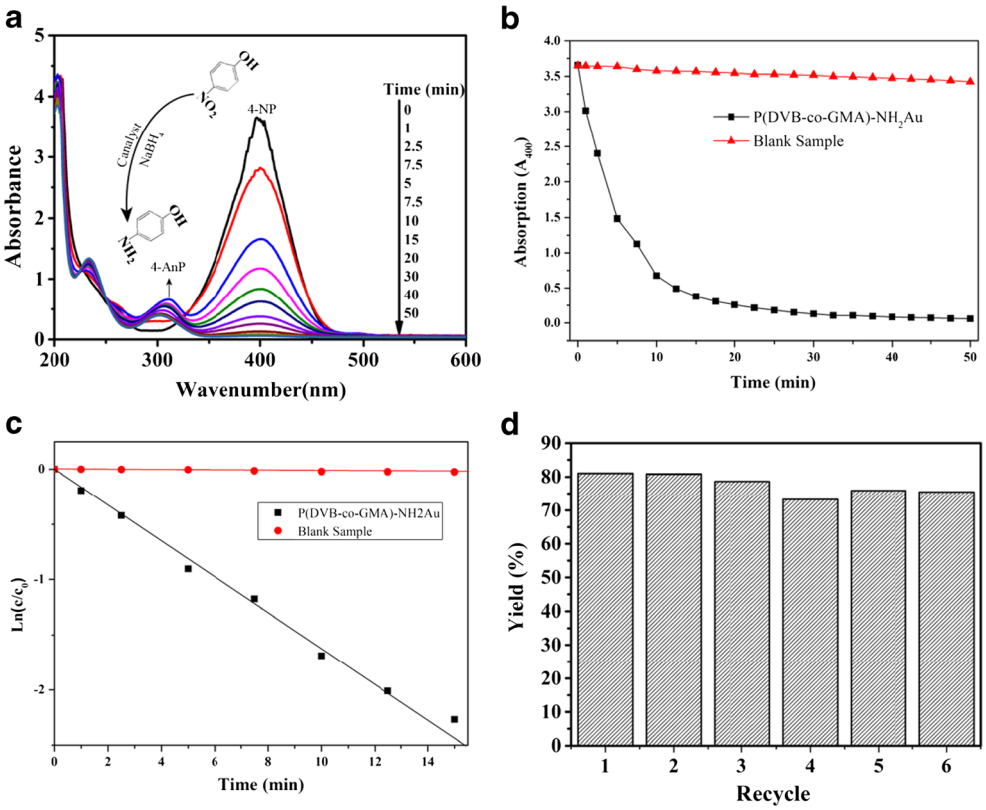

Fig. 7 Catalytic performance of P(DVB-*co*-GMA)-NH_2@Au for the reduction of 4-NP to 4-AnP: **a** UV–vis spectra of the catalytic systems at different times, the inserted scheme refers the reaction; **b** the relationship between the concentration of 4-NP and ln(C/C0) vs the reaction time; and **c** recycled catalytic property; and D yields of 4-AnP after each cycle

of 4-NP to 4-AnP was slightly decreased from 82.0 % for the first cycle to 77.0 % for the sixth one. This meant that 93.9 % of the catalytic activity of P(DVB-*co*-GMA)-NH_2@Au remained after recycling for five times, indicating that the supported gold nanocolloids had a good stability and facile recyclability as a catalyst. The excellent recyclability was mainly contributed from the efficient protection of the amino groups to Au NPs in the gel layer of P(DVB-*co*-GMA)-NH_2@Au, which was similar to the case of the grafted polyamidoamine (PAMAM) dendrimers-stabilized Au NPs in our previous work [26]. In the present work, P(DVB-*co*-GMA)-NH_2@Au microspheres were fixed on the wall of the tube during centrifugation for recovery of the supported catalyst to prevent loss of the catalyst during recovery.

Conclusion

Narrow disperse P(DVB-*co*-GMA) microspheres with epoxy groups having the average diameters from 1.37 to 2.91 μm were prepared by distillation precipitation copolymerization with GMA fraction ranging from 0 to 0.70 (*V*/*V*) in DVB and GMA feed. The P(DVB-*co*-GMA) microspheres had the highest loading capacities of the epoxy groups as 2.05 mmol/g, which were highly reactive and accessible to be transferred into the amino groups via the surface modification with ethylene diamine. The P(DVB-*co*-GMA)-NH_2@Au with an average size of 4.53 nm gold nanocolloids were prepared by the in situ reduction of $HAuCl_4$ with sodium borohydrate as reductant via the efficient complexing interaction between the nitrogen atom of the amino group and gold atom. The polymer microsphere-stabilized gold nanocolloids exhibited a stable and facilely recoverable activity for the catalytic reduction of 4-NP to 4-AnP in an aqueous solution.

Acknowledgments This work was supported by the Natural Science Foundation of China (grant nos. 21174065, 21374049, and 21344004), PCSIRT (IRT1257), and Tianjin Higher Education Science and Technology Fund Planning Project (project no. 20110506).

References

1. Weng LH, Rostamzadeh R, Nooryshokry N, Le HC, Golzarian J (2013) In vitro and in vivo evaluation of biodegradable embolic microspheres with tunable anticancer drug release. Acta Biomater 9:6823–6833
2. Horak D, Babic M, Mackova H, Benes MJ (2007) Preparation and properties of magnetic nano- and microsized particles for biological and environmental separations. J Sep Sci 30:1751–1772
3. Liu B, Wang XM, Zhao YW, Yang XL (2013) Polymer shell as a protective layer for the sandwiched gold nanoparticles and their recyclable catalytic property. J Colloid Interface Sci 395:91–98
4. Grinou A, Yun YS, Jin HJ (2012) Polyaniline nanofiber-coated polystyrene/graphene oxide core-shell microsphere composites. Macromol Res 20:84–92

5. Bai F, Li R, Yang XL, Li SN, Huang WQ (2006) Preparation of narrow-dispersion or monodisperse polymer microspheres with active hydroxyl group by distillation–precipitation polymerization. Polym Int 55:319–325
6. Li SF, Yang XL, Huang WQ (2005) Preparation of monodisperse crosslinked polymer microspheres having chloromethyl group by distillation precipitation polymerization. Chin J Polym Sci 23:197–202
7. Zhang WJ, Piao SH, Choi HJ (2013) Facile and fast synthesis of polyaniline-coated poly(glycidyl methacrylate) core-shell microspheres and their electro-responsive characteristics. J Colloid Interface Sci 402:100–106
8. Senkal BF, Bicak N (2001) Glycidyl methacrylate based polymer resins with diethylene triamine tetra acetic acid functions for efficient removal of Ca(II) and Mg(II). React Funct Polym 49:151–157
9. Ma ZY, Guan YP, Liu HZ (2005) Synthesis and characterization of micron-sized monodisperse superparamagnetic polymer particles with amino groups. J Polym Sci A Polym Chem 43:3433–3439
10. Tsai HA, Chen CH, Lee WC (2001) Influence of surface hydrophobic groups on the adsorption of proteins onto nonporous polymeric particles with immobilized metal ions. J Colloid Interface Sci 240: 379–383
11. Li X, Liu Y, Xu Z, Yan HS (2011) Preparation of magnetic microspheres with thiol-containing polymer brushes and immobilization of gold nanoparticles in the brush layer. Eur Polym J 47:1877–1884
12. Moszner N, Salz U (2001) New developments of polymeric dental composites. Prog Polym Sci 26:535–576
13. Saatchi K, Haefeli UO (2009) Radiolabeling of biodegradable polymeric microspheres with $[Tc\text{-}99m(CO)_3]^+$ and in vivo biodistribution evaluation using microSPECT/CT imaging. Bioconjug Chem 20: 1209–1217
14. Lee J, Yun HS (2014) Hydroxyapatite-containing gelatin/chitosan microspheres for controlled release of lysozyme and enhanced cytocompatibility. J Mater Chem B 2:1255–1263
15. Horowitz D, Margel S, Shimoni T (1985) Iron detoxification by haemoperfusion through deferoxamine-conjugated agarose-polyacrolein microsphere beads. Biomaterials 6:9–16
16. Zheng MM, Dong L, Lu Y, Guo PM, Deng QC, Li WL, Feng YQ, Huang FH (2012) Immobilization of Candida rugosa lipase on magnetic poly(allyl glycidyl ether-co-ethylene glycol dimethacrylate) polymer microsphere for synthesis of phytosterol esters of unsaturated fatty acids. J Mol Catal B 74:16–23
17. Chaleawlert-Umpon S, Pimpha N (2012) Preparation of magnetic polymer microspheres with reactive epoxide functional groups for direct immobilization of antibody. Colloids Surf A 414:66–74
18. Wang RW, Zhang Y, Ma GH, Su ZG (2006) Preparation of uniform poly(glycidyl methacrylate) porous microspheres by membrane emulsification-polymerization technology. J Appl Polym Sci 102: 5018–5027
19. Ma ZY, Guan YP, Liu XQ (2005) Preparation and characterization of non-porous superparamagnetic microspheres with epoxy groups by dispersion polymerization. Chin J Chem Eng 13:239–243
20. Zhou WQ, Gu TY, Su ZG, Ma GH (2007) Synthesis of macroporous poly(glycidyl methacrylate) microspheres by surfactant reverse micelles swelling method. Eur Polym J 43:4493–4502
21. Suzuki D, Kawaguchi H (2005) Gold nanoparticle localization at the core surface by using thermosensitive core-shell particles as a template. Langmuir 21:12016–12024
22. Imoata Y, Wada T, Handa H, Fujimoto K, Kawaguchi H (1994) Preparation of DNA-carrying affinity latex and purification of transcription factors with the latex. J Biomater Sci Polym Ed 5:293–302
23. Horak D, Shapoval P (2000) Reactive poly(glycidyl methacrylate) microspheres prepared by dispersion polymerization. J Polym Sci A Polym Chem 38:3835–3863
24. Ma NN, Ma C, Wang NY, Li CY, Elingarami S, Mou XB, Tang YJ, Zheng S, He NY (2014) Application of functional microsphere in human hepatitis B virus surface antigen detection. J Nanosci Nanotechnol 14:3348–3355
25. He J, Lu YC, Luo GS (2014) Ca(II) imprinted chitosan microspheres: an effective and green adsorbent for the removal of Cu(II), Cd(II) and Pb(II) from aqueous solutions. Chem Eng J 244:202–208
26. Li PF, Yang LR, He XQ, Wang J, Kong P, Xing HF, Liu HZ (2012) Synthesis of PGMA microspheres with amino groups for high-capacity adsorption of Cr(VI) by cerium initiated graft polymerization. Chin J Chem Eng 20:95–104
27. Feng HL, Zhang RN, Yang XL (2013) Synthesis of P(MBA-*co*-MAA) microsphere-grafted PAMAM dendrimers and their application as supporters for gold nanoparticles. Colloid Polym Sci 291: 1329–1339
28. Dong XQ, Zheng YH, Huang YB, Chen XS, Jing XB (2010) Synthesis and characterization of multifunctional poly(glycidyl methacrylate) microspheres and their use in cell separation. Anal Biochem 405:207–212
29. Kundu P, Heidari H, Bals S, Ravishankar N, van Tendeloo G (2014) Formation and thermal stability of gold-silica nanohybrids: insight into the mechanism and morphology by electron tomography. Angew Chem Int Ed 53:3970–3974
30. Theil F, Dellith A, Dellith J, Undisz A, Csaki A, Fritzsche W, Popp J, Rettenmayr M, Dietzek B (2014) Ru dye functionalized Au-SiO_2@TiO_2 and Au/Pt-SiO_2@TiO_2 nanoassemblies for surface-plasmon-induced visible light photocatalysis. J Colloid Interface Sci 421:114–121
31. Petryayeva E, Krull UJ (2012) Quantum dot and gold nanoparticle immobilization for biosensing applications using multidentate imidazole surface ligands. Langmuir 28:13943–13951
32. Liu B, Zhang DW, Wang JC, Chen C, Yang XL, Li CX (2013) Multilayer magnetic composite particles with functional polymer brushes as stabilizers for gold nanocolloids and their recyclable catalysis. J Phys Chem C 117:6363–6372
33. Liu B, Sun SX, Gao ZB, Bian GM, Qi YL, Li CX (2014) Silica-g-poly[2-(*N*,*N*-dimethyl amino) ethyl methacrylate] hybridnanospheres with polymer brushes as stabilizer for metallicnanocolloids. Colloids Surf A 456:195–202
34. Bai F, Yang XL, Huang WQ (2004) Synthesis of narrow or monodisperse poly(divinylbenzene) microspheres by distillation-precipitation polymerization. Macromolecules 37:9746–9752
35. Liu GY, Yang XL, Wang YM (2007) Silica/poly(*N*,*N*′-methylenebisacrylamide) composite materials by encapsulation based on a hydrogen-bonding interaction. Polymer 48:4385–4392
36. Lu XY, Huang D, Yang XL, Huang WQ (2006) Preparation of narrow or monodisperse polymer microspheres with cyano group by distillation-precipitation polymerization. Polym Bull 54:171–178
37. Gao CY, Zhang H, Wu M, Liu Y, Wu YP, Yang XL, Feng XZ (2012) Polyethyleneimine functionalized polymer microsphere: a novel delivery vector for cells. Polym Chem 3:1168–1173
38. Bai F, Yang XL, Li R, Huang B, Huang WQ (2006) Monodisperse hydrophilic polymer microspheres having carboxylic acid groups prepared by distillation precipitation polymerization. Polymer 47: 5775–5784
39. Yang P, Zhao Y, Lu Y, Xu QZ, Xu XW, Dong L, Yu SH (2011) Phenol formaldehyde resin nanoparticles loaded with CdTe quantum dots: a fluorescence resonance energy transfer probe for optical visual detection of copper(II) ions. ACS Nano 5:2147–2154
40. Liu W, Yang XL, Huang WQ (2006) Catalytic properties of carboxylic acid functionalized polymer microsphere-stabilized gold metallic colloids. J Colloid Interface Sci 304:160–165
41. Liu W, Yang XL, Xie L (2007) Size-controlled gold nanocolloids on polymer microsphere-stabilizer via interaction between functional groups and gold nanocolloids. J Colloid Interface Sci 313:494–502
42. Zhou L, Gao C, Hu X, Xu W (2011) General avenue to multifunctional aqueous nanocrystals stabilized by hyperbranched polyglycerol. Chem Mater 23:1461–1470

43. Henry CR (1998) Surface studies of supported model catalysts. Surf Sci Rep 31:231–325
44. Koga H, Kitaoka T (2011) One-step synthesis of gold nanocatalysts on a microstructured paper matrix for the reduction of 4-nitrophenol. Chem Eng J 168:420–425
45. Ma XX, Zhu YH, Li LC, Wang CS, Lu XH, Yang ZH (2012) Thermal stability of gold catalyst supported on mesoporous titania nanofibers. Chin J Catal 33:1480–1485
46. Li XL, Zhu XH, Fang YY, Yang HL, Zhou YC, Chen WM, Jiao LX, Huo HF, Li R (2014) Programmed synthesis of magnetic mesoporous silica nanotubes with tiny Au nanoparticles: a highly novel catalyst system. J Mater Chem A 2:10485–10490
47. Yang HL, Li SW, Zhang XY, Wang XY, Ma JT (2014) Imidazolium ionic liquid-modified fibrous silica microspheres loaded with gold nanoparticles and their enhanced catalytic activity and reusability for the reduction of 4-nitrophenol. J Mater Chem A 2:12060–12067